



Effect of the Addition of Mesogenic Thiol Ligand Modified Gold Nanoparticles on the Thermal Stabilization of Blue Phases

Jihye Lee, Sung-Kyu Hong & Hyun Jung

To cite this article: Jihye Lee, Sung-Kyu Hong & Hyun Jung (2015) Effect of the Addition of Mesogenic Thiol Ligand Modified Gold Nanoparticles on the Thermal Stabilization of Blue Phases, *Molecular Crystals and Liquid Crystals*, 606:1, 134-143, DOI: 10.1080/15421406.2014.915663

To link to this article: <http://dx.doi.org/10.1080/15421406.2014.915663>



View supplementary material [↗](#)



Published online: 15 Jan 2015.



Submit your article to this journal [↗](#)



Article views: 95



View related articles [↗](#)



View Crossmark data [↗](#)

Effect of the Addition of Mesogenic Thiol Ligand Modified Gold Nanoparticles on the Thermal Stabilization of Blue Phases

JIHYE LEE,¹ SUNG-KYU HONG,² AND HYUN JUNG^{1,*}

¹Department of Chemistry, Advanced Functional Nanohybrid Material Laboratory, Dongguk University Seoul-campus, Jung-gu, Seoul, Korea

²Department of Chemical & Biochemical Engineering, Dongguk University Seoul-campus, Jung-gu, Seoul, Korea

In this paper, we introduce surface modified gold nanoparticles with mesogenic thiol ligands in liquid crystal, for expansion of the temperature range of blue phases (BPs). We have used polarized optical microscope and UV-vis spectrophotometer to identify the thermal stabilization of BPs. The BPs range of nanoparticles doped liquid crystal is significantly dependent upon the addition amount of gold nanoparticles, and the molar ratios of attached ligands [4'-(10-mercaptodecyloxy)biphenyl-4-carbonitrile and dodecanethiol]. This study could provide a new and facile strategy to stabilize BPs, from the aspect of the surface modification of nanoparticles.

Keywords Blue phases; expansion of temperature range; mesogenic thiol ligand; surface modified gold nanoparticles; 4'-(10-mercaptodecyloxy)biphenyl-4-carbonitrile

Introduction

Blue phases (BPs) have captivated attention due to their unique optical properties, and great potential applications as three-dimensional lasers [1], fast-light modulators [2], and self-assembling tunable photonic devices [3]. However, BPs appear within a very narrow temperature range, of normally less than one degree Celsius, between the cholesteric (Ch) and isotropic (Iso) phases [4]. This obstacle comes from line defects existing in the crystalline lattice of BPs. The BP structure contains double twist cylinders of cholesteric liquid crystal molecules. Depending upon the orientation of these cylinders in three-dimensional space, BPs are classified into BPI, BPII, and BPIII, which correspond to the crystalline nature of body-centered cubic, simple cubic, and amorphous, respectively [5–7]. When the cylinders meet along three perpendicular directions for the construction of BPs, disclination line defects inevitably form, due to topological constraints. Thus, BPs have a limited thermal stability within a narrow temperature range, due to the free-energy cost of disclination.

To expand the temperature range of BPs, various stabilizing agents have been adapted in the BPs system, such as a bimesogen chiral mixture, or different polymers [4, 8, 9]. These

*Address correspondence to Hyun Jung, Advanced Functional Nanohybrid Material Laboratory, Department of Chemistry, Dongguk University Seoul-campus, 30 Pildong-ro 1-gil, Jung-gu, Seoul 100-715, Korea. E-mail: chemphile@dongguk.edu

Color versions of one or more of the figures in the article can be found online at www.tandfonline.com/gmcl.

approaches have been realized to widen the temperature range of the BPs, by polymerizing disclination lines, and by using a flexoelectricity of twin molecules, and a chiral compound having molecular biaxiality. However, these approaches have suffered from field induced phase transition, high driving voltage, large switching hysteresis, and long term stability [10]. More recently, various types of nanoparticles, such as Au, CdSe, and aerosils, have been introduced, as a means of stabilizing BPs [11–13]. According to the recent theoretical investigation by Žumer et al., nanoparticles involved BPs can use the disclination lines as trapping sites. Their theoretical results show that nanoparticles with size of around 40 nm could easily be trapped in disclination lines of BPs. After the trapping of nanoparticles, the volume and free energy associated with disclination reduce and hence stabilize the BPs [14].

In the present study, therefore, primary attention is paid to the expansion of temperature range for BPs, by the introduction of mesogenic thiol ligand modified gold nanoparticles into the disclination lines. For this purpose, liquid-crystalline thiol ligands were prepared *via* an organic synthetic route [15], and surface modified gold nanoparticles were synthesized through Brust's two-phase reaction [16] with the prepared mesogenic ligands. The expansion of temperature range of BPs is systematically investigated, depending upon the addition amount of gold nanoparticles, and the molar ratios of mesogenic thiol ligands and alkyl thiol ones, for searching for the optimal interaction between the gold nanoparticles and disclination lines in BPs.

Experimental Section

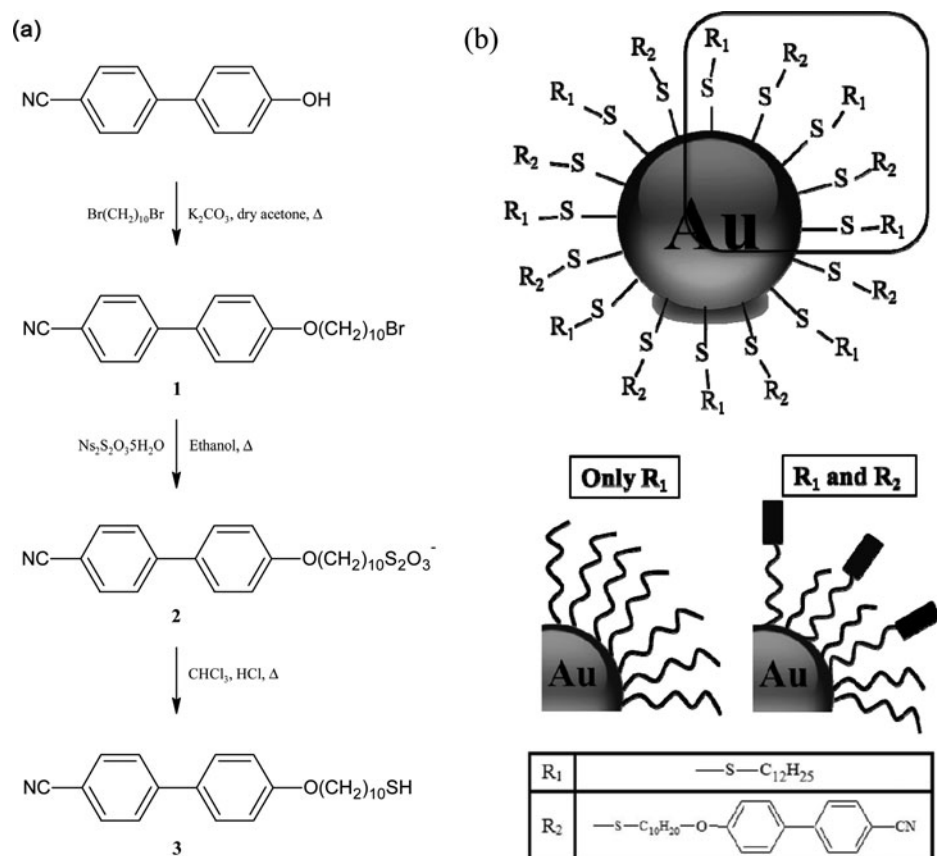
Synthesis of Mesogenic Thiol Ligand

(4'-(10-mercaptopodecyloxy)biphenyl-4-carbonitrile, HS10OCB)

The mesogenic thiol ligand, HS10OCB (**3**), was prepared by the organic synthetic route previously described [15] with some modification, from 4'-hydroxy-4-biphenylcarbonitrile, through the three steps indicated in Scheme 1(a). First, 4'-(10-bromodecyloxy)biphenyl-4-carbonitrile (**1**) was obtained by alkylation of 4'-hydroxy-4-biphenylcarbonitrile (0.50 g, 2.56 mmol) in the presence of excess 1,10-dibromodecane (7.68 g, 25.6 mmol). Then, the obtained 4'-(10-bromodecyloxy)biphenyl-4-carbonitrile (0.33 g, 1.0 mmol) (**1**) was transformed to Bunte salt (**2**), by reacting with sodium thiosulfate pentahydrate (0.27 g, 1.07 mmol). Finally, HS10OCB (**3**) was obtained, by the hydrolysis of the obtained Bunte salt (**2**). The final product was confirmed by nuclear magnetic resonance (NMR) spectroscopy, using Bruker Ascend 500 NMR spectrometer. ¹H NMR (CDCl₃): δ (ppm) 6.99–7.70 (m, 8 H, aromatic H), 4.00 (t, 2 H, CH₂O), 2.53 (q, 2H, CH₂S), 1.35 (t, 1 H, SH), 1.4–1.9 (m, 16 H, aliphatic CH₂).

Preparation of Mesogenic Thiol Ligand Modified Gold Nanoparticles

Surface modified gold nanoparticles were synthesized *via* Brust's two-phase reaction, in the presence of the obtained mesogenic thiol ligands. An aqueous solution (30 ml) of HAuCl₄·3H₂O (0.12 g, 0.3 mmol) and a solution of tetraoctylammonium bromide (TOAB) (0.33 g, 0.6 mmol) in toluene (80 ml) were mixed with vigorous stirring, until the yellow aqueous solution became colorless, and the organic phase turned orange color. To obtain various molar ratios of HS10OCB modified gold nanoparticles, the ligands of different molar ratios of HS10OCB to the entire thiol ligands (0.00, 0.13, 0.20, and 0.50) were dissolved in toluene (10 ml). Then, thiol ligands (0.3 mmol) dissolved toluene



Scheme 1. (a) Synthesis process of HS10OCB and (b) schematic description for surface modified gold nanoparticle with HS10OCB and dodecanethiol.

solution was added in two-phase mixed solution, and stirred for 10 min. Subsequently, a fresh aqueous solution (30 ml) of sodium borohydride (0.11 g, 3 mmol) was added dropwise. The organic phase immediately turned to ruby red, and was further stirred for 4 hr. The organic layer was separated and washed three times with distilled water. The synthesized gold nanoparticles were collected using centrifuge and washed three times with ethanol and toluene to remove excess TOAB and thiol ligands. Finally, mesogenic thiol ligands modified gold nanoparticles were obtained as dark brown precipitation, and then redispersed in toluene (Scheme 1(b)). The obtained gold nanoparticles are referred to hereafter as Au1, Au2, Au3, and Au4, according to the molar ratios of HS10OCB to the entire thiol ligands 0.00, 0.13, 0.20, and 0.50 during the preparation process. Morphological characterization of the obtained gold nanoparticles was done using JEOL JEM-3010 high resolution-transmission electron microscope (HR-TEM).

Preparation of Samples for Temperature Range Observation

A chiral nematic liquid crystal mixture were prepared for pure BPs without gold nanoparticles, by mixing the 4'-pentyl-4-biphenylcarbonitrile (5CB) (46.25 wt%, Sigma-Aldrich),

JC-1041XX (46.25 wt%, JNC Corp.), and ISO-(6OBA)₂ (7.5 wt%, synthesized by laboratory) at 80°C. Chiral nematic liquid crystal mixtures with gold nanoparticles were obtained by adding 1 wt%, 3 wt%, and 5 wt% of gold nanoparticles in liquid crystal mixtures. The mixture solution was stirred at 90°C for complete removal of solvent, and additionally dried under vacuum for overnight. Subsequently, the obtained mixture was filled into 10 μm gap sandwich cell by capillary forces in the isotropic phase. The temperature range of BPs for each sample was evaluated using polarizing optical microscope (POM) (Nikon Eclipse LV100 POL) with a hot stage (Linkam LTS 420) under crossed Nicoles, while cooling and heating the samples at a rate of 0.1°C/min. Additionally, the reflection spectra of the samples were observed with multichannel photo-detector (Hamamatsu C4564-010G) to ensure the temperature range of BPs. The reflection spectra were corrected after holding the sample for 15 min at each temperature, to prevent the effect of thermal hysteresis during the cooling process. As the light source, xenon lamp was used for the reflection spectra observations.

Results and Discussion

High Resolution Transmission Electron Microscopy Measurements

To observe the size of the obtained nanoparticles, we measured the HR-TEM. Figure 1 represents HR-TEM images and histograms of the size distribution, for surface modified gold nanoparticles as a function of molar ratios of HS10OCB and dodecanethiol. Depending upon the increase of the molar ratio of HS10OCB/entire thiol ligands from 0.00 to 0.50, the mean diameters and standard deviations of the obtained nanoparticles were 1.9 ± 0.8 , 2.8 ± 0.4 , 2.9 ± 0.6 , and 2.8 ± 0.5 nm, as displayed in Figs. 1(a)–(d), respectively. The size distribution of nanoparticles was determined by statistically analyzing the individual

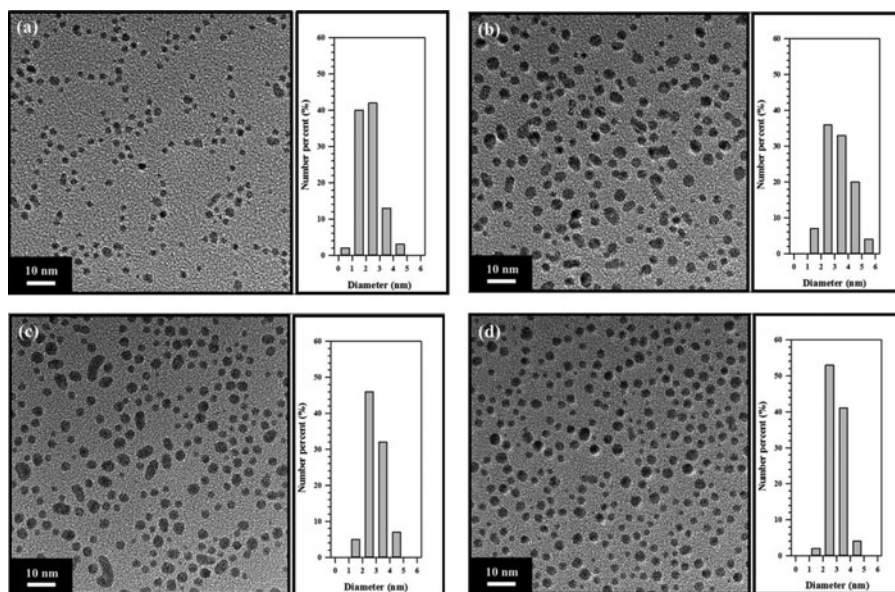


Figure 1. HR-TEM images and histograms of the obtained gold nanoparticles (a) Au1, (b) Au2, (c) Au3, and (d) Au4.

Table 1. Temperature range of BPs, depending upon the addition amount of Au4 on cooling, by POM observation

Amount of gold nanoparticles (wt%)	Phase transition temperature (°C) on cooling		
	$T_{\text{Iso-BP}}$	$T_{\text{BP-Ch}}$	ΔT_{BP}
1	45.8	42.5	3.3
3	42.7	39.1	3.6
5	44.8	41.7	3.1

diameters of at least 100 particles in the obtained HR-TEM images. The HR-TEM results are significant from two aspects. First, the size of the obtained nanoparticles is appropriate to be trapped in the disclination lines, which have an approximate diameter of 40 nm [14]. Second, nanoparticles were successfully modified with different molar ratio of HS10OCB and dodecanethiol with similar size. These results indicate that the main effect on the expansion of temperature range for BPs comes from the interaction between the surface modified nanoparticles, and disclination lines in BPs.

Polarizing Optical Microscope Observation

In order to measure the effect of the concentration of gold nanoparticles on the BPs range, we observe the phase transition temperatures of the different concentrations of gold nanoparticles dispersed samples using a POM during the cooling process, as displayed in Fig. S2. The phase transition temperatures of liquid-crystalline mixture introduced with different concentration of Au4 are listed in Table 1. When the surface modified gold nanoparticles were introduced with 1 wt%, 3 wt%, and 5 wt% in liquid crystals, the temperature ranges of BPs while cooling process, were 3.2, 3.6, and 3.1°C, respectively. The further addition of gold nanoparticles shows not only significant reduction of BPs temperature ranges, but also enhancement of aggregation of each nanoparticle [17, 18].

According to the defect theory, the free energy around defects of BPs decreases on the introduction of surface elasticity, and also BPs can be stabilized by nonliquid crystal materials, through the replacing of the volume occupied by the disclination lines [8, 11, 19]. Previous theoretical simulation results show that nanoparticles dispersed BPs can be

Table 2. Temperature range of BPs, depending upon the molar ratios of HS10OCB on heating and cooling by POM observation

Molar ratios of HS10OCB	Phase transition temperature (°C) on heating			Phase transition temperature (°C) on cooling		
	$T_{\text{Ch-BP}}$	$T_{\text{BP-Iso}}$	ΔT_{BP}	$T_{\text{Iso-BP}}$	$T_{\text{BP-Ch}}$	ΔT_{BP}
0.00	40.2	41.8	1.6	41.4	39.4	2.0
0.13	44.3	45.8	1.5	46.5	43.3	3.2
0.20	43.7	46.5	2.8	46.3	41.7	4.6
0.50	41.5	43.1	1.6	42.7	39.1	3.6

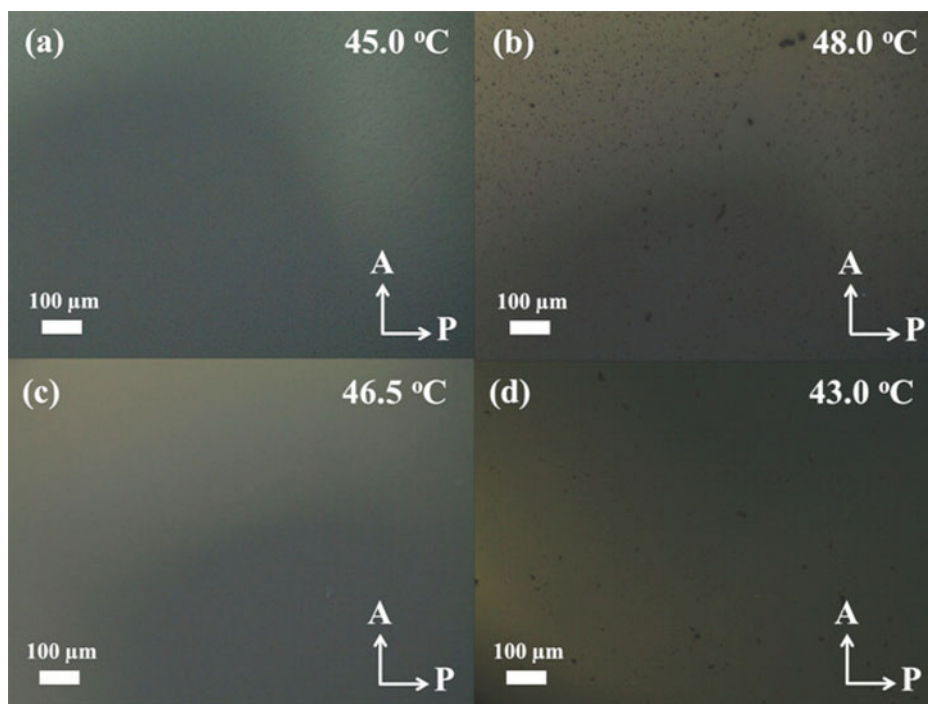


Figure 2. POM images of isotropic phase, in different gold nanoparticles [(a) Au1, (b) Au2, (c) Au3, and (d) Au4] dispersed samples.

trapped in the disclination lines as a result of elastic interactions [14]. Therefore, we could infer that the addition of surface modified gold nanoparticles plays a role in reducing the volume and the free energy around the disclination line of BPs. Although the volume and the free energy around the disclinations could be continuously suppressed, with increasing the concentration of gold nanoparticles, the BPs structure would be disordered and destabilized, above the optimal concentration.

To investigate the effect of the surface property of gold nanoparticles on the BPs ranges, we observed the phase transition temperatures of 3 wt% gold nanoparticles, with different molar ratio of mesogenic thiol ligand and dodecanethiol ligand (Au1-Au4) dispersed samples, using a POM during the heating and cooling process as summarized in Table 2, and detailed POM images are shown in Fig. S3–S6. The BPs ranges of the cooling process are wider than those of the heating process, due to the super-cooling of the BPs [20]. When the molar ratio of HS10OCB is increased from 0.00 to 0.20, the samples show an increasing BPs range with the widest to 4.6°C; whereas, further increase of the HS10OCB suppresses the BPs range. Base on this phenomenon, we can estimate that the surface nature of gold nanoparticles critically influences the stabilization of the BPs, by the optimal interaction between the gold nanoparticles and disclinations. Figure 2 represents the images of isotropic phase, in the different gold nanoparticles (Au1-Au4) dispersed samples. In particular, Au3 (molar ratio of HS10OCB is 0.20) nanoparticles are finely dispersed in liquid crystals (Fig. 2(c)), in comparison to the Au1, Au2, and Au4 dispersed samples (Figs. 2(a)–(d)). The latter samples tended to form self-assembled large aggregates of gold nanoparticles, due to the strong inter-particle interaction, leading to the nature of the surface property of nanoparticles.

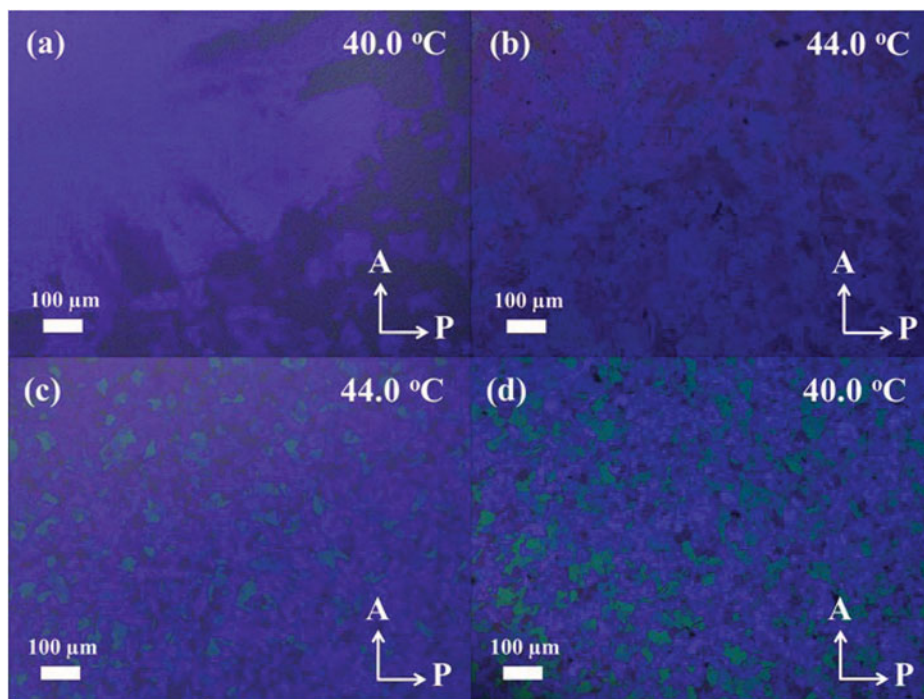


Figure 3. POM images of BP, in different gold nanoparticles [(a) Au1, (b) Au2, (c) Au3, and (d) Au4] dispersed samples.

The POM images of BP for 3 wt% gold nanoparticles with different molar ratio of HS10OCB dispersed samples are displayed in Fig. 3. For all images, typical mosaic platelet textures were observed, similar to normal cubic BPs [11]. When the molar ratio of HS10OCB is increased from 0.00 to 0.20, the colored domains in the BPs become smaller (Figs. 3(a)–(c)); whereas, further increase of HS10OCB shows that colored domains in the BPs grew (Fig. 3(d)). Upon cooling from isotropic to BPs, spherical droplets of liquid crystal uniformly formed, gradually grew, and finally disappeared. As the size of the droplets increased, the dark contours gradually merged, and clearly emerged. At the end of the transition, the fringe disappeared, and produced only platelet BP texture (Figs. S5(a)–(g)). From these results, we suggest that gold nanoparticles modified with 0.20 molar ratio of HS10OCB show enhanced stability of BPs, owing to the optimal interaction between gold nanoparticles and disclination lines. HS10OCB ligand has a biphenyl functional moiety that is expected to strongly interact with liquid crystal molecule through the π – π interaction. But this interaction might be hindered by steric and geometric limitation in our system. In this regards, 0.20 molar ratio of HS10OCB attached nanoparticles show the best stability of BPs. With further cooling below 41.7°C, a focal conic texture of cholesteric phase began to appear (Fig. S5(h)).

UV Spectra Observation

The BPs show sensitive light reflection on Bragg diffraction of the cubic lattice in the visible spectrum [21, 22]. So, we measured the selective reflection of BPs to more clearly identify

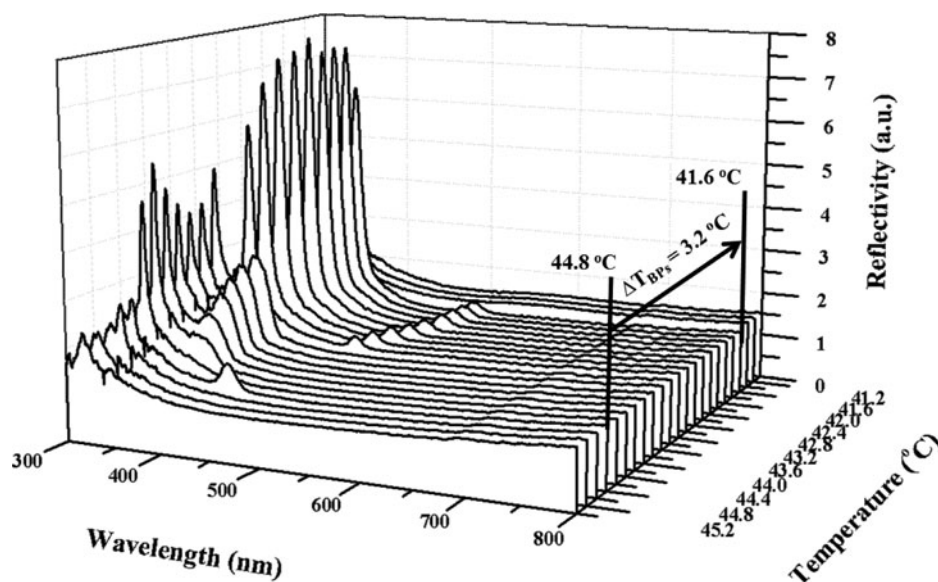


Figure 4. UV-vis reflection spectra of Au3 dispersed sample as a function of temperature during the cooling process.

the temperature range of the gold nanoparticles dispersed samples. Figure 4 represents the reflection spectra of Au3 dispersed sample, depending upon the temperature. The detailed phase sequence of the obtained samples is listed in Table 3. In the isotropic phase, a reflection peak did not appear. Upon cooling below phase transition temperature from isotropic to BPs, a reflection peak corresponding to the diffraction was exhibited at 348~373 nm. As a function of temperature, the reflection intensity of the BPs was changed. A strong reflection peak appeared during the 3.2°C, between 41.6°C and 44.8°C. Moreover, the reflection peak of BPs shifted toward the longer wavelength, from 348 nm to 373 nm, with decreasing temperature. Another small peak appearing at around 500 nm was attributed to the local surface plasmon resonance (LSPR) of the gold nanoparticles [23], which is a red-shift with decreasing temperature, because the LSPR is known to red-shift, when the particles become larger, or form aggregates [24]. Although the temperature ranges of BPs by UV-vis spectrophotometer observation were slightly narrower than those obtained by

Table 3. BPs range depending upon the molar ratios of HS10OCB on cooling by UV-vis spectrophotometer observation

Molar ratios of HS10OCB	Phase transition temperature (°C) on cooling		
	$T_{\text{Iso-BP}}$	$T_{\text{BP-Ch}}$	ΔT_{BP}
0.00	40.3	38.7	1.6
0.13	44.6	42.6	2.0
0.20	44.8	41.6	3.2
0.50	40.8	38.6	2.2

POM measurements, the patterns of molar ratios dependency of thiol ligands were quite similar.

Conclusion

In summary, we have successfully synthesized the mesogenic thiol ligand *via* an organic synthetic route, and prepared surface modified gold nanoparticles, through the Brust's two-phase reaction with the obtained mesogenic ligands. The expansion of the temperature range of BPs is systematically investigated, depending upon the addition amount of gold nanoparticles, and the molar ratios of HS10OCB. According to the POM study, all of the gold nanoparticle dispersed samples exhibited expansion of the BPs range. From the UV-vis reflection spectroscopy results, the widest BPs range of nanoparticle doped liquid crystal is 3.2°C, by the addition of 3 wt% gold nanoparticles, modified with 0.20 molar ratio of HS10OCB. On the basis of the above results, a model for the surface modification of nanoparticles is proposed, in which the critical mixing ratio of ligands for the optimal interaction between nanoparticles and disclination lines provides an expansion of the BPs range.

Funding

This research was supported by Leading Foreign Research Institute Recruitment Program and Basic Science Research Program through the National Research Foundation of Korea (NRF) funded by the Ministry of Education, Science and Technology (MEST) (No. 2013-044975) and the Ministry of Education (No. NRF-2013R1A1A2013035).

Supplemental Data

Supplemental data for this article can be accessed at www.tandfonline.com/gmcl.

References

- [1] Cao, W. Y., Munoz, A., Palfy-Muhoray, P., & Taheri, B. (2002). *Nat. Mater.*, *1*, 111.
- [2] Moreira, M. F., Carvalho, I. C. S., Cao, W., Bailey, C., Taheri, B., & Palfy-Muhoray, P. (2004). *Appl. Phys. Lett.*, *85*, 2691.
- [3] Vijayaraghavan, R. K., Abraham, S., Rao, D. S. S., Prasad, S. K., & Das, S. (2010). *Chem. Commun.*, *46*, 2796.
- [4] Coles, H. J., & Pivnenko, M. N. (2005). *Nature*, *436*, 997.
- [5] Barbet-Massin, R., Cladis, P. E., & Pieranski, P. (1984). *Phys. Rev. A*, *30*, 1161.
- [6] Dubois-Violette, E., Pansu, B., & Pieranski, P. (1990). *Mol. Cryst. Liq. Cryst.*, *192*, 221.
- [7] Koistinen, E. P., & Keyes, P. H. (1995). *Phys. Rev. Lett.*, *74*, 4460.
- [8] Kikuchi, H., Yokota, M., Hisakado, Y., Yang, H., & Kajiyama, T. (2002). *Nat. Mater.*, *1*, 64.
- [9] Hisakado, Y., Kikuchi, H., Nagamura, T., & Kajiyama, T. (2005). *Adv. Mater.*, *17*, 96.
- [10] Wong, J. M., Hwang, J. Y., & Chien, L. C. (2011). *Soft Matter*, *7*, 7956.
- [11] Yoshida, H., Tanaka, Y., Kawamoto, K., Kubo, H., Tsuda, T., Fujii, A., Kuwabata, S., Kikuchi, H., & Ozaki, M. (2009). *Appl. Phys. Express*, *2*, 121501.
- [12] Karatairi, E., Rozic, B., Kutnjak, Z., Tzitzios, V., Nounesis, G., Cordoyiannis, G., Thoen, J., Glorieux, C., & Kralj, S. (2010). *Phys. Rev. E*, *81*, 041703.
- [13] Rozic, B., Tzitzios, V., Karatairi, E., Tkalec, U., Nounesis, G., Kutnjak, Z., Cordoyiannis, G., Rosso, R., Virga, E. G., Musevic, I., & Kralj, S. (2011). *Eur. Phys. J.*, *34*, 17.
- [14] Ravnik, M., Alexander, G. P., Yeomans, J. M., & Zumer, S. (2010). *Faraday Discuss*, *144*, 159.
- [15] Kumar, S. K., P. S. (2005). *Liq. Cryst.*, *32*, 659.

- [16] Brust, M., Walker, M., Bethell, D., Schiffrin, D. J., & Whyman, R. (1994). *J. Chem. Soc., Chem. Commun.*, 7, 801.
- [17] Sharma, A., Worden, M., & Hegmann, T. (2012). *Ferroelectrics*, 431, 154.
- [18] Wang, L., He, W. L., Xiao, X., Meng, F. U., Zhang, Y., Yang, P. Y., Wang, L. P., Xiao, J. M., Yang, H., & Lu, Y. F. (2012). *Small*, 8, 2189.
- [19] He, W. L., Pan, G. H., Yang, Z., Zhao, D. Y., Niu, G. G., Huang, W., Yuan, X. T., Guo, J. B., Cao, H., & Yang, H. (2009). *Adv. Mater.*, 21, 2050.
- [20] Dierking, I., Blenkhorn, W., Credland, E., Drake, W., Kociuruba, R., Kayser, B., & Michael, T. (2012). *Soft Matter*, 8, 4355.
- [21] Dmitrienko, V. E. (1989). *Liq. Cryst.*, 5, 847.
- [22] Gerber, P. R. (1985). *Mol. Cryst. Liq. Cryst.*, 116, 197.
- [23] Duff, D. G., Baiker, A., & Edwards, P. P. (1993). *J. Chem. Soc., Chem. Commun.*, 1, 96.
- [24] Muhlig, S., Rockstuhl, C., Yannopapas, V., Burgi, T., Shalkevich, N., & Lederer, F. (2011). *Opt. Express*, 19, 9607.